INDERSCIENCE PUBLISHERS
Linking academia, business and industry through research

International Journal of Environment and Sustainable Development

ISSN online: 1478-7466 - ISSN print: 1474-6778
https://www.inderscience.com/ijesd

Dynamic monitoring and evolution of urban green space landscape sustainability based on spatiotemporal analysis algorithm

Liping Ouyang, Yichen He, Zufan Chen, Ke He

DOI: 10.1504/IJESD.2025.10073738

Article History:

Received:	31 March 2025
Last revised:	26 July 2025
Accepted:	21 August 2025
Published online:	23 February 2026

Dynamic monitoring and evolution of urban green space landscape sustainability based on spatiotemporal analysis algorithm

Liping Ouyang

School of Digital Media and Interaction Design,
Guangzhou Maritime University,
Guangzhou, 510000, Guangdong, China
Email: 13397520328@163.com

Yichen He*

China Faculty of Arts and Humanities,
University of Macau,
Macau, 100084, Macau, China
Email: 15011927287@163.com
*Corresponding author

Zufan Chen

School of Art and Design,
Guangzhou Institute of Science and Technology,
Guangzhou, 510000, Guangdong, China
Email: 13729872860@163.com

Ke He

School of Architecture and Art,
Guangdong Lingnan Institute of Technology,
Guangzhou, 510000, Guangdong, China
Email: 1079933066@qq.com

Abstract: To address the issue of disconnect between the spatial-temporal characteristics of urban green space landscape dynamics and sustainability assessment, this study utilises the spatial-temporal DBSCAN (ST-DBSCAN) algorithm to identify hotspot areas of green space coverage changes and the spatial-temporal variations in green space fragmentation, and combines this with a geographically weighted regression (GTWR) model to quantitatively analyse the impact of driving factors such as population growth and land development intensity on the ecological service functions of green spaces. The experimental results show that the LSTM+ST-ConvNet model predicts the green space area for 2020-2024 with an error of only 50 square kilometres, outperforming other prediction models such as ARIMA, XGBoost, and Random Forest (the ARIMA model had an error of 70 square kilometres). This model can more accurately predict trends in green space area changes, providing theoretical support for urban green space.

Keywords: urban green landscape; geographically and temporally weighted regression; spatial-temporal DBSCAN; dynamic monitoring; ecological function; urban green space; UGS; change vector analysis; CVA.

Reference to this paper should be made as follows: Ouyang, L., He, Y., Chen, Z. and He, K. (2026) 'Dynamic monitoring and evolution of urban green space landscape sustainability based on spatiotemporal analysis algorithm', *Int. J. Environment and Sustainable Development*, Vol. 25, No. 5, pp.3–23.

Biographical notes: Liping Ouyang holds a landscape architecture doctorate from the Cheongju University, South Korea. She is currently employed as an Associate Professor at the Guangzhou Maritime University, with a main research focus on spatial environment and landscape planning.

Yichen He is a student majoring in Portuguese Studies at the University of Macau. He has obtained excellent grade in his course and received several scholarships, including the Jorge Alvares Foundation Scholarship, BNU UM Affinity Card Scholarship and UM RC Foundation Scholarship. He also participated in various competitions and won awards, including the first prize of 2023 writing competition "My notion of cultural safety" held by the Macau government, champion of 2023 UM Portuguese Debating Contest and excellence award in the 8th World Chinese-Portuguese Translation Competition.

Zufan Chen received his Bachelor's degree from the Hubei Normal University in China. Currently, he is working at the School of Art and Design, Guangzhou Institute of Science and Technology. His research interest includes artistic design, environmental design and digital modelling.

Ke He holds a Master's in Engineering from the Xi'an Engineering University. He is currently serving as the Honorary Dean and an Associate Professor of the School of Architecture and Art at Guangdong Lingnan Vocational and Technical College, with a main research focus on visual communication design and landscape art engineering.

1 Introduction

As the global urbanisation process accelerates, urban green space (UGS), as an important part of the ecosystem, plays an irreplaceable role in improving the environment, regulating the climate, and improving the quality of life of residents. Urban expansion and changes in land use (Roy et al., 2022) have led to a continuous reduction in green space area, fragmentation of green space structure, and degradation of ecological functions, which seriously affect the sustainable development of cities. Climate change, population growth, political control, and many other factors have increased the complexity and dynamic changes of urban green landscapes (Chen et al., 2022; Jian and Hao, 2020). Traditional static research methods cannot fully reveal the laws of its evolution and stability. Spatiotemporal analysis algorithms can analyse the spatial changes of UGS from different perspectives, identify the spatial distribution pattern and temporal evolution trend of green landscapes, and provide decision support for green city planning and management.

Current research focuses on static assessment and lacks in-depth analysis of the relationship between spatiotemporal dynamic evolution and sustainability. Therefore, the unique contribution of this paper lies in integrating the spatial-temporal DBSCAN (ST-DBSCAN) and geographically and temporally weighted regression (GTWR) models to identify hot spots of green space changes and quantify the spatiotemporal non-stationarity of driving factors. The constructed 'landscape evolution-ecological function degradation' dynamic correlation model provides accurate decision-making support for the restoration and resilience improvement of high-density UGS. Specifically, this paper uses the ST-DBSCAN algorithm to systematically analyse the spatiotemporal differentiation characteristics of UGS landscapes, which can automatically identify hot spots of green coverage changes and reflect the spatiotemporal evolution of green space landscape fragmentation. By considering the local weighted effects of space and time, the GTWR model can accurately discover the changes in ecological service functions in different regions and periods. This paper reveals the intrinsic connection between green space landscape changes and ecological function degradation by constructing a dynamic correlation model between green space landscape evolution and ecological function degradation. The dynamic monitoring of green space evolution provides theoretical support and decision-making basis for optimising ecological functions and improving the resilience of UGS systems, and promotes the sustainable management of UGSs. This study applied spatiotemporal analysis algorithms to dynamically monitor and evaluate the ecological functions of UGSs, expanding the application of spatiotemporal analysis methods in environmental science, urban ecology, and other fields. This has promoted the development of spatiotemporal analysis methods in urban ecosystem research and proposed new ideas and methods for future research in the field of UGS landscape.

2 Related works

With the acceleration of urbanisation, the problem of UGS vegetation fragmentation is becoming increasingly serious. The study of UGS is of great significance for ensuring the sustainability of urban ecosystems, improving the quality of life of urban residents, and promoting the construction of green cities. To identify and analyse the current status of urban vegetation fragmentation around the world, Kowe et al. (2021) used remote sensing technology, Landsat data, and a discrete landscape pattern index to monitor UGS landscape and vegetation fragmentation. To solve the problem of estimating the complexity of evapotranspiration in UGSs with limited water resources, Nouri et al. (2020) used satellite images of different spatial resolutions and a method based on vegetation index, and linked remote sensing ET (evapotranspiration) with ground ET data through artificial neural networks. In order to solve the problem of UGS changes caused by human activities, Nasehi used thematic mapper (TM) and Enhanced Thematic Mapper Plus (ETM+) satellite images. By calculating different landscape indicators using FRAGSTATS software, he analysed the landscape change trends and fragmentation processes in Tehran District 2, revealing the trend of building land replacing green space and landscape fragmentation (Nasehi and Imanpour Namin, 2020). To analyse the impact of rapid urbanisation on urban green infrastructure and hydrological and meteorological disasters, Ghalehteimouri et al. (2024) evaluated land use changes and their impacts on urban forests, urban water value changes, and flood frequency by analysing the normalised difference vegetation index (NDVI) and normalised difference water index

(NDWI) of remote sensing images, combined with Markov chain, ArcGIS, and TerrSet software. In order to study the water resource management of UGSs under climate warming and drought conditions, Kuhlemann used isotope tracers in precipitation and soil water and traditional hydrological measurement methods. He evaluated the water distribution and evapotranspiration processes under different types of UGSs in Berlin, Germany, and explored the impact of different vegetation types on urban water resources (Kuhlemann et al., 2021). Although the above studies have adopted a variety of methods to evaluate the impact of UGS on the ecological environment, it is still necessary to study the sustainability of UGS landscapes based on more advanced technologies such as spatiotemporal analysis algorithms.

Based on the excellent analysis capabilities of spatiotemporal analysis algorithms in time and space, they are widely used in UGS research. To address the issue of the relationship between physical activity in urban parks and park characteristics, Tao et al. (2024) used the GTWR model to analyse the seasonal and daily changes in physical activity in Shanghai urban parks through a series of cross-sectional surveys, providing a scientific basis for urban planners and park designers to promote an active and sustainable urban environment. In order to solve the problem of insufficient estimation accuracy of biological vegetation volume in urban unit attached green space, Li proposed an living vegetation volume (LVV) estimation scheme based on backpack lidar point cloud data. He achieved high-precision estimation of UGS LVV by eliminating multi-scale ground point cloud, clustering with DBSCAN (Density-Based Spatial Clustering of Applications with Noise), extracting plant point cloud with PointNet++ network model, extracting canopy point cloud, and calculating single tree canopy LVV with the convex hull method (Li et al., 2022). To address the issue of spatial differences in UGSs and their socioeconomic relationship with surrounding communities, Yang (2020) used geographic information systems combined with spatial statistical methods such as optimised hotspot analysis, network analysis, and spatiotemporal clustering analysis to provide urban planners with a spatial evaluation basis based on the benefits of green space utilisation. To solve the problem of the relationship between land use change and population growth and migration, Naikoo et al. (2020) used K-means clustering technology to classify land use, combined with change detection technology and statistical analysis, to provide a scientific basis for understanding the urbanisation process and its environmental impact. In order to solve the problem of detecting spatiotemporal correlation patterns of complex geographical phenomena, He proposed a spatiotemporal correlation pattern detection framework based on complex events, which represents complex geographical events through hierarchical modelling and directed spatiotemporal path data structure. He combined sequential analysis technology and adaptive algorithms to detect the spatiotemporal patterns of events, revealing the spatiotemporal patterns of the distribution of complex geographical phenomena and their possible driving forces (He et al., 2020). The above methods have solved many traditional research problems in predicting future green space trends, detecting dynamic changes, analysing evolution laws, and mining association rules, providing new technical means and theoretical support for UGS landscape research. This paper proposes a more comprehensive research framework and method that integrates a multidimensional evaluation system and a deep learning algorithm.

3 Construction and implementation of spatiotemporal analysis framework

3.1 Data collection and pre-processing

This paper collected remote sensing images of UGSs (Lv et al., 2022) to ensure the comprehensiveness and timeliness of the data used in the study. This study selected Landsat series satellite images (Lv et al., 2022), which included historical image data of Guangdong Province, to ensure the period and spatial coverage of the data (the time range is from 2010 to 2025, and the imagery has a spatial resolution of 30 metres. Landsat data was chosen for its global coverage, long time series archive, and free and open access). The remote sensing images of some green space types are shown in Figure 1.

Figure 1 Remote sensing images of some types of green space, (a) production green space (b) ecological green space (c) green belt (d) disaster prevention green space (e) public green space (see online version for colours)

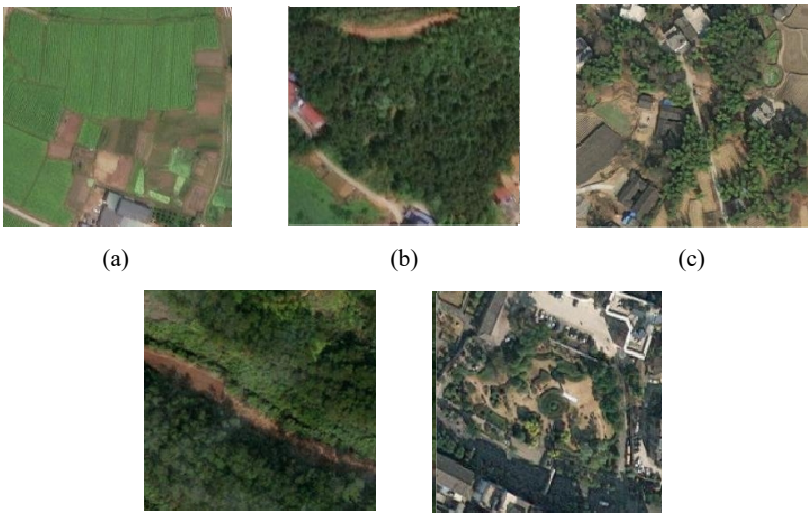

(a) (b) (c)

(d) (e)

Figure 1 depicts remote sensing images of five types of green space, namely production green space, ecological green space, green belt, disaster prevention green space, and public green space. Production green space is used for production activities such as agriculture, gardening, and forestry, and can provide food and natural resources needed by urban residents. Ecological green space mainly undertakes the functions of ecological protection, improving environmental quality, and promoting biodiversity. In order to improve the accuracy and reliability of remote sensing images, the images are pre-processed, including radiation correction (García-Cabrera et al., 2020), atmospheric correction, geometric correction, etc. The radiation correction uses the Fmask algorithm (Candra et al., 2020) to remove the effects of clouds and shadows to ensure the accuracy of green space coverage in the image. The radiation correction formula is:

$$L_{\text{cal}} = G \cdot (DN - \text{Offset}) + \text{Bias} \tag{1}$$

G is the gain factor, and Offset is the offset value.

Atmospheric correction is performed using the 6S model, and the formula is:

$$\rho = \frac{L_{\text{ref}}}{E_{\text{sun}}} \cdot \cos(\theta) \tag{2}$$

Among them, ρ is the reflectivity after atmospheric correction, L_{ref} is the reflected brightness, E_{sun} is the solar irradiance, and θ is the solar zenith angle. After atmospheric correction, the interference of the atmosphere on remote sensing reflection is eliminated, and the restoration of ground object information is improved. Geometric correction uses high-precision control points to perform coordinate transformation to eliminate geometric deformation caused by satellite orbit and ground errors. To ensure that data from different sources are compared and analysed in the same dimension, this paper normalises all image data to make its value between 0 and 1 for NDVI (Huang et al., 2021) in remote sensing image data, thus ensuring the comparability of the data. This is a standardisation step performed after the above corrections are completed. Its purpose is to unify the comparability of data from different phases, rather than replacing atmospheric correction. The calculation formula of NDVI is:

$$NDVI = \frac{NIR - RED}{NIR + RED} \tag{3}$$

Among them, NIR is the reflectance of the near-infrared band, and RED is the reflectance of the red band. NDVI values range from –1 to +1, with higher values indicating denser vegetation cover and better health, while lower values generally indicate a lack of vegetation or poor vegetation health.

Figure 2 Schematic diagram of the random data enhancement method (see online version for colours)

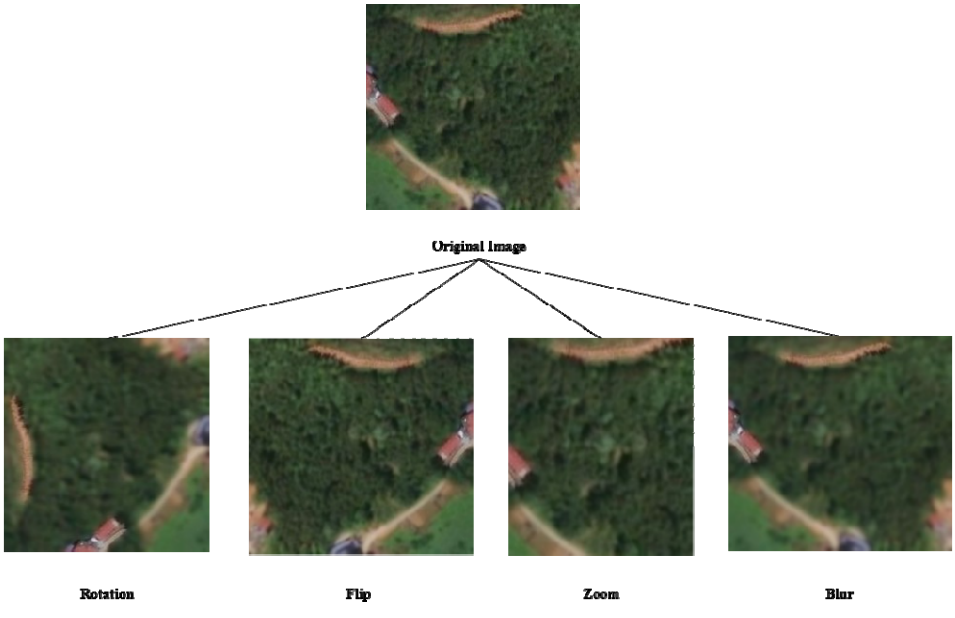

In order to improve the overall quality of samples and prevent underfitting problems caused by insufficient samples during training, data enhancement technology is used to increase the number of training samples. This paper mainly enhances samples in four ways: rotation, flipping, zooming, and blurring. Figure 2 shows a schematic diagram of the random enhancement method for sample data.

The distribution of the pre-processed dataset is shown in Table 1.

Table 1 Dataset distribution

Green space type	*Training data*	*Test data*	*Total*
Public green space	735	245	980
Ecological green space	774	258	1,032
Leisure green space	792	264	1,056
Green belt	705	235	940
Production green space	819	273	1,092
Landscape green space	768	256	1,024
Disaster prevention green space	780	260	1,040
Functional green space	813	271	1,084
Educational and cultural green space	717	239	956

Table 1 shows the distribution of the dataset. According to the functions of UGSs, they are divided into nine types of green spaces, and the total number of data samples for each type is not much different. These nine types of green spaces are public green spaces, ecological green spaces, leisure green spaces, green belts, production green spaces, landscape green spaces, disaster prevention green spaces, functional green spaces, and educational and cultural green spaces. The total number of samples of production green spaces is 1,092, which is the largest number of samples among all types.

Oversampling and cost-sensitive learning were used to balance the nine types of green space training samples. A bias test was then performed, and the confusion matrix showed that the difference in F1-score of each type was less than 3%, proving that the classification bias was controllable.

3.2 Spatial-temporal clustering analysis to identify hotspots

There is a disconnect between the spatiotemporal differentiation characteristics and sustainability assessment in the dynamic evolution of UGS landscapes. With the acceleration of urbanisation, UGSs are facing multiple environmental and human impacts. These changes not only show complex spatial heterogeneity but also present different spatiotemporal evolution laws. This paper introduces the ST-DBSCAN algorithm to accurately identify hotspots of green space increase and decrease by clustering the spatiotemporal distribution of UGS landscapes.

In the ST-DBSCAN algorithm, spatial and temporal neighbourhoods are defined to perform density clustering on each point, and the radius is determined by combining the spatial scale of the study area, data resolution, and the typical period of green space change (Howarth et al., 2021). The calculation formula for spatial distance is:

$$d_s\left(p_i, p_j\right) = \sqrt{\left(x_i - x_j\right)^2 + \left(y_i - y_j\right)^2} \tag{4}$$

In formula (4), $d_s(p_i, p_j)$ represents the distance between points p_i and p_j in space, and x_i and x_j are the spatial coordinates of points p_i and p_j, respectively.

$$d_t(p_i, p_j) = |t_i - t_j| \tag{5}$$

In formula (5), $d_t(p_i, p_j)$ represents the time difference between points p_i and p_j in time, and t_i and t_j are the timestamps of points p_i and p_j, respectively.

When the two points meet the neighbourhood conditions in both space and time, the spatiotemporal distance between the two points is:

$$d_{st}(p_i, p_j) = \sqrt{(x_i - x_j)^2 + (y_i - y_j)^2} + |t_i - t_j| \le \epsilon \tag{6}$$

A core point is a point whose number of points in the neighbourhood is greater than or equal to the minimum number of points. The determination formula is:

$$\text{CorePoint}(p_i) = \text{Count}(p_i) \ge \text{MinPts} \tag{7}$$

The boundary point is the point number in the space-time neighbourhood that is less than the minimum number of points, and the judgement formula is:

$$\text{BorderPoint}(p_i) = \text{Count}(p_i) < \text{MinPts and } \exists p_j \in \mathcal{N}(p_i), \text{CorePoint}(p_j) \tag{8}$$

Among them, $N(p_i)$ represents the spatiotemporal neighbourhood of point p_i.

Noise points are those points that are neither core points nor boundary points. Noise points do not belong to any cluster. The judgement formula is:

$$\text{NoisePoint}(p_i) = \text{Count}(p_i) < \text{MinPts and } \forall p_j \in \mathcal{N}(p_i), \text{CorePoint}(p_j) \tag{9}$$

After point type identification, the clustering process is carried out. By expanding the neighbourhood of the core point, the high-density areas are gradually divided into the same cluster. The cluster expansion formula is:

$$\mathcal{C}(p_i) = \{p_j \mid d_{st}(p_i, p_j) \le \epsilon \text{ and CorePoint}(p_j)\} \tag{10}$$

After clustering is completed, the hot spots of green space changes are identified according to the spatial distribution of clusters. Through the analysis of spatiotemporal change patterns, it is further confirmed which areas have significant increases or decreases in green space. After identifying the hot spots of green space, the spatiotemporal differentiation of green space fragmentation is further analysed. Fragmentation analysis reveals the changing trend of green space spatial structure by measuring the number, area, connectivity, and other characteristics of green space patches. The fragmentation of green space is usually manifested as an increase in the number of green space patches. The fragmentation trend can be determined by calculating the change in the number of green space patches in different periods. The formula for calculating the number of green space patches is:

$$\text{PatchCount}(t) = \text{Number of patches at time } t \tag{11}$$

The degree of green space fragmentation is quantified by calculating the connectivity of green space patches. The connectivity index is the average patch contact degree, and the calculation formula for the average patch contact degree is:

$$ACA = \frac{\sum_{i=1}^{N} A_i}{A_{\text{total}}} \tag{12}$$

Among them, A_i is the area of the patch, and A_{total} is the total area of the entire green area. The smaller the ACA value, the higher the degree of fragmentation.

In the clustering results, high-density clusters correspond to hot spots where green space changes dramatically (such as areas with sudden area reduction). The spatiotemporal differentiation characteristics of fragmentation are quantified by calculating the number of green space patches in each cluster [formula (11)] and the connectivity index [formula (12)].

The fragmentation rate is usually measured by calculating the rate of change of green area. With the advancement of urbanisation, the rate of reduction of green area usually shows an accelerating trend. The formula for calculating the rate of change of fragmentation is:

$$\text{Fragmentation Rate} = \frac{A_{initial} - A_{final}}{T_{final} - T_{initial}} \tag{13}$$

In formula (13), $A_{initial}$ and A_{final} represent the green area at the initial and final time points, respectively, and T_{final} and $T_{initial}$ represent the corresponding times. Through the spatiotemporal clustering of the ST-DBSCAN algorithm, the hotspots of urban green landscape changes can be identified. Through detailed analysis of core steps such as spatial neighbourhood, temporal neighbourhood, and density calculation, accurate spatiotemporal data support is provided for dynamic monitoring, protection, and restoration of green spaces.

3.3 Filling missing data with spatiotemporal interpolation

In order to fill the missing values in remote sensing data, this paper adopts the spatiotemporal Kriging interpolation method (Gao et al., 2023), taking into account the correlation of spatial and temporal dimensions, thereby generating a continuous spatiotemporal data set.

For spatial and temporal correlation, this paper uses the following spatiotemporal semivariogram (Goovaerts et al., 2024) model:

$$\gamma(h, \tau) = \sigma^2 \left[\left(\frac{h}{a_s} \right)^{\alpha} + \left(\frac{\tau}{a_t} \right)^{\beta} \right] \text{b} \tag{14}$$

$\gamma(h, \tau)$ represents the semivariogram value under the spatial distance h and time difference τ, and σ^2 is the variance term, which represents the overall variability of the data. a_s and a_t are the spatial and temporal scale parameters, respectively, indicating the relevant range in the spatial and temporal dimensions. α and β are used to describe the degree of change in space and time.

After the space-time covariance model is established, Kriging interpolation is used for data prediction. In space-time Kriging interpolation, the values of missing points are estimated by weighted averaging based on the data values of known points and their spatial and temporal distances from the missing points. The basic formula of Kriging interpolation is:

$$Z^*(p_0) = \sum_{i=1}^{N} \lambda_i Z(p_i) \tag{15}$$

In formula (15), $Z^*(p_0)$ represents the predicted value of the missing point p_0, $Z(p_i)$ is the observed value of the known point p_i, and λ_i is the weight coefficient related to the spatial and temporal relationship of the known point p_i, which is usually calculated by solving the covariance matrix.

The weight coefficient is solved by a linear equation system based on the covariance matrix. The solution formula of the covariance matrix is:

$$\mathbf{C} = \begin{bmatrix} \gamma(h_1, \tau_1) & \gamma(h_1, \tau_2) & \cdots & \gamma(h_1, \tau_N) \\ \gamma(h_2, \tau_1) & \gamma(h_2, \tau_2) & \cdots & \gamma(h_2, \tau_N) \\ \vdots & \vdots & \vdots & \vdots \\ \gamma(h_N, \tau_1) & \gamma(h_N, \tau_2) & \cdots & \gamma(h_N, \tau_N) \end{bmatrix} \tag{16}$$

3.4 Spatiotemporal regression model to analyse driving factors

In order to reveal the complex relationship between the spatiotemporal evolution of UGS changes and its driving factors, this paper adopts the GTWR model. The GTWR model is an improved model that combines geographically weighted regression (Comber et al., 2023; Yu et al., 2020) and spatiotemporal weighted regression (Wu et al., 2021). It can handle spatiotemporal heterogeneity and quantify the spatiotemporal impacts of multiple driving factors (such as population density, temperature change, land policy, etc.) on green space changes. The GTWR model can analyse the non-stationary impact of different driving factors on UGS changes in both spatial and temporal dimensions.

The specific driving factors included in the model include: population density (derived from the city statistical yearbook and gridded population distribution data, reflecting the pressure of population expansion on green space), land development intensity [calculated based on land use/land cover change (LULC) classification data to calculate the proportion or change rate of construction land, representing the direct occupation of green space resources by urbanisation], regional economic development level (such as per capita GDP, derived from the statistical yearbook, related to the city's development investment capacity), temperature change (derived from meteorological station observation data or reanalysis data, reflecting the stress of climate change on vegetation growth), precipitation (same source temperature data, measuring the impact of moisture conditions on the ecological function of green space), and key land policy implementation time nodes (such as ecological protection red line demarcation, large park construction planning, etc. introduced as virtual variables or time series intensity indicators, derived from government planning documents and announcements, used to quantify the effect of policy intervention). All spatial data have been matched with a unified coordinate system and spatial resolution, (e.g., resampled to the same grid as the remote sensing image), time series data have been aligned with the green space change observation period, and necessary standardisation or normalisation has been performed to eliminate dimensional effects, ensuring that data from different sources and types can be integrated into a unified spatiotemporal analysis framework.

The spatiotemporal weight function formula of the GTWR model is:

$$Y_{i,t} = \beta_0 (s_i, t) + \sum_{j=1}^{m} \beta_j (s_i, t) X_{i,j,t} + \epsilon_{i,t} \tag{17}$$

GTWR uses spatial and temporal weighting functions to perform weighted regression analysis on sample data.

The spatial weighting function reflects the correlation between data points in space, while the temporal weighting function describes the influence relationship between data points in the time dimension. In the GTWR model, the spatial weighting function uses the Gaussian weighting function, while the temporal weighting function is weighted based on time differences. The spatial weighting function W_s and the temporal weighting function W_t are defined as:

$$W_s = \exp\left(-\frac{d(s_i, s_j)^2}{2h_s^2} \right) \tag{18}$$

$$W_t = \exp\left(-\frac{(t_i - t_j)^2}{2h_t^2} \right) \tag{19}$$

$d(s_i, s_j)$ is the distance between spatial cells s_i and s_j. H_s is the spatial bandwidth parameter, which is used to control the range of spatial weighting. H_t is the temporal bandwidth parameter, which is used to control the range of temporal weighting. The spatial and temporal weighting functions weight the sample data in the regression model so that samples closer to the current point contribute more to the regression results, while samples farther from the current point contribute less.

The estimation of regression coefficients is the core of the GTWR model, which is solved by the least squares method. At each spatial unit and time point, the regression coefficients are estimated locally. The specific calculation formula is as follows:

$$\hat{\beta}(s_i, t) = \left(X^T W(s_i, t) X \right)^{-1} X^T W(s_i, t) Y \tag{20}$$

In formula (20), X is a matrix containing all independent variables (driving factors). $W(s_i, t)$ is a spatial and temporal weighted matrix, which incorporates spatial and temporal weighted information into the regression analysis. Y is an observation value vector, which represents the actual change data of UGS.

Through this regression equation, the regression coefficient of each spatial unit and time point can be obtained, revealing the spatiotemporal impact of various driving factors on green space changes.

3.5 Change vector analysis (CVA) to detect dynamic changes in green space

The dynamic evolution of the UGS landscape, this paper introduces the CVA algorithm (Zakeri and Saradjian, 2022) to detect the area change and spatial transfer characteristics of green space in different periods. Difference images are obtained for the green space change amplitude of green space coverage images at different time points. The green space change amplitude can be calculated by the following formula:

$$D_{i,j} = \left| C_{i,j}(t_2) - C_{i,j}(t_1) \right| \tag{21}$$

$D_{i,j}$ represents the change amplitude of green space at spatial position (i, j) between periods t_1 and t_2. The change vector is calculated by quantifying the change amplitude of the difference image to reflect the spatial transfer mode of green space coverage change. The change vector of each spatial unit is calculated in the following way:

$$V_{i,j} = \left(D_{i,j}(t_2) - D_{i,j}(t_1)\right) \cdot \Delta t \tag{22}$$

Among them, $V_{i \text{ and } j}$ represent the change vector, which reflects the size and direction of the green space change.

After calculating the change vector, the spatial transfer characteristics of the green space are further analysed. Through the different states of green space from increase, decrease, to transfer, the dynamic evolution process of the UGS landscape is reflected. Spatial transfer characteristic analysis quantifies the spatial law of green space change through spatial autocorrelation coefficient and variation index, and further reveals the spatiotemporal characteristics of green space change patterns. Spatial autocorrelation analysis measures the concentration and distribution pattern of green space change in space through Moran's I coefficient (Westerholt, 2023). Moran's I coefficient reflects the correlation degree of green space changes in adjacent spatial units. Its formula is as follows:

$$I = \frac{n\sum_{i,j} w_{ij}\left(X_i - \bar{X}\right)\left(X_j - \bar{X}\right)}{\sum_i \left(X_i - \bar{X}\right)^2} \tag{23}$$

The value range of I is [–1, 1]. When $I > 0$, it means that the green space change has positive spatial autocorrelation, that is, the change trends of adjacent areas are similar; when $I < 0$, it means that the green space change has negative spatial autocorrelation, that is, the change trends of adjacent areas are opposite.

After completing the spatial autocorrelation analysis, this paper classified the change patterns of green spaces into four basic patterns: green space increase, green space decrease, green space maintenance, and green space transfer. The spatial distribution of these change patterns can reveal the spatiotemporal characteristics of UGS landscapes, such as which areas of green space show an expansion trend and which areas show a degradation or transfer trend.

3.6 Spatiotemporal prediction model predicts future trends

In order to accurately predict the future change trend of the UGS landscape, this paper adopts a spatiotemporal prediction (Zhang et al., 2023) model based on long short-term memory (LSTM) and spatio-temporal convolutional network (ST-ConvNet). This model can capture the spatiotemporal characteristics of UGS based on historical data, and then accurately predict future trends.

The LSTM model structure includes an input layer (time series of green space coverage data), multiple LSTM layers (capturing long-term dependencies in time series), a fully connected layer (feature mapping), and an output layer (predicting green space changes). The prediction formula is:

$$\hat{Y}_{t+1} = f_{LSTM}\left(X_1, X_2, ..., X_T\right) \tag{24}$$

$\hat{Y}_{t+1}$ is the predicted green space change value, and f_{LSTM} represents the mapping function of the LSTM model.

ST-ConvNet converts green space coverage data into spatiotemporal data and uses multiple convolutional layers to perform operations in the spatial and temporal dimensions to extract local spatial features and temporal dependencies. Its architecture includes an input layer, a convolution layer, a pooling layer, a fully connected layer, and an output layer, and finally predicts the changes of green space at future time points. The prediction formula of the ST-ConvNet model is:

$$\hat{Y}_{t+1} = f_{ST\text{-}ConvNet}\left(X_{1,x,y}, X_{2,x,y}, ..., X_{T,x,y}\right) \tag{25}$$

In formula (25), $\hat{Y}_{t+1}$ is the predicted green space change value, and $f_{ST\text{-}ConvNet}$ represents the mapping function of the ST-ConvNet model.

4 Evaluation indicators and calculation methods

4.1 Green space coverage

Calculate green space coverage, that is, the ratio of the number of pixels in the green space area to the number of pixels in the total area:

$$GreenCover = \frac{Area_{Green}}{Area_{Total}} \tag{26}$$

4.2 Green space change rate

The green space change rate is used to evaluate the expansion or degradation speed of green space and is an important indicator for measuring the dynamic changes of UGS. To calculate the green space change rate, this paper selects remote sensing images at multiple time points, analyses the changes in green space area between different time points, and uses the difference method to calculate the changes in green space area:

$$\Delta Area = Area_t - Area_{t-1} \tag{27}$$

Calculate the green space change rate based on the area and time interval of change:

$$ChangeRate = \frac{\Delta Area}{t-(t-1)} \tag{28}$$

Among them, t is the current time point, and $t - 1$ is the previous time point.

4.3 Sustainability index

The sustainability index comprehensively considers the green area, ecological function, and change trend, and is used to evaluate the long-term sustainability of the green landscape. In this study, a multi-factor weighted model was constructed, taking green space coverage, change rate, ecological service value, and spatial heterogeneity as inputs to calculate a comprehensive sustainability index:

$$SustainabilityIndex = w_1 \times GreenCover + w_2 \times ChangeRate + w_3 \times ESV + w_4 \times SpatialHeterogeneity \quad (29)$$

In formula (29), *GreenCover* is the green space coverage, *ChangeRate* is the green space change rate, *ESV* is the ecological service value, and *SpatialHeterogeneity* is the spatial heterogeneity index. The weights were determined based on principal component analysis, reflecting the dominant contribution of ecosystem service value to sustainability (loading 0.87), and their robustness was verified through sensitivity analysis.

5 Experimental design

5.1 Evaluation of UGS change rate

The experiment takes eight major cities in Guangdong Province as the research objects (based on their urbanisation rate, green coverage change rate and climate zoning for screening to ensure that the samples represent high, medium, and low development intensity areas). The experimental process includes collecting remote sensing image data in 2010, 2015, 2020, and 2025 in stages, calculating the changes in green area of each city, extracting green area using normalised vegetation index, calculating the green area change rate, and standardising it to eliminate seasonal effects. The experimental results show the speed of expansion or degradation of green space in each city, providing a scientific basis for UGS management. The experimental results are shown in Table 2.

Table 2 Green space area and green space change rate of each city from 2010 to 2025

City	*Green area in 2010 (km^2)*	*Green area in 2015 (km^2)*	*Green area in 2020 (km^2)*	*Green area in 2025 (km^2)*	*Green space change rate (2010–2015)*	*Green space change rate (2015–2020)*	*Green space change rate (2020–2025)*
Shenzhen	270	290	310	320	+7.41%	+6.90%	+3.23%
Zhuhai	110	115	120	125	+4.55%	+4.35%	+4.17%
Foshan	150	160	165	170	+6.67%	+3.13%	+3.03%
Shantou	80	85	90	92	+6.25%	+5.88%	+2.22%
Shaoguan	45	50	55	60	+11.11%	+10.00%	+9.09%
Huizhou	120	125	130	135	+4.17%	+4.00%	+3.85%
Meizhou	85	90	95	100	+5.88%	+5.56%	+5.26%
Yangjiang	75	80	85	90	6.67%	6.25%	5.88%

Table 2 describes the green area data of eight cities in Guangdong Province in 2010, 2015, 2020, and 2025, as well as the green area change rates from 2010 to 2015, 2015 to 2020, and 2020 to 2025. Among them, Shenzhen and Shaoguan had relatively high green area change rates of 7.41% and 11.11% respectively, from 2010 to 2015, with obvious green area expansion, which is closely related to their urbanisation process, greening construction, and ecological restoration projects promoted by the government. Zhuhai and Huizhou have a low rate of change in green space between 2010 and 2025, with the rate of change remaining between 3% and 5%. The green space area has also increased, but the growth rate is significantly lower than that of other cities, which may be due to

the squeeze on the green space area by land development and infrastructure construction. This experiment shows that the difference in the rate of change of green space in different cities in Guangdong Province provides a quantitative basis for the planning and management of UGS.

Figure 3 Predictions of green area in 2020–2024 by various models (see online version for colours)

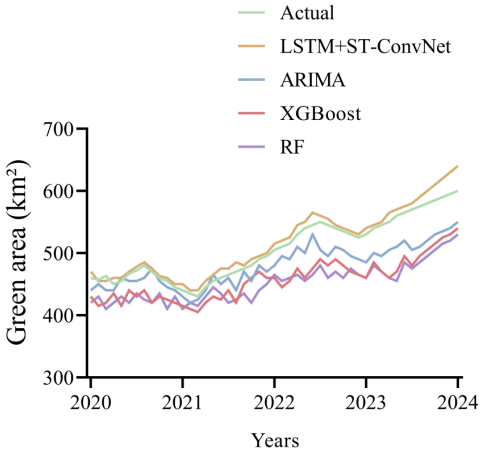

5.2 Green space area prediction experiment

This experiment predicts the green area of Guangzhou through a variety of spatiotemporal prediction models and evaluates its prediction accuracy. Accurately predicting the changing trend of green areas can help urban planners formulate reasonable green space protection and development strategies, optimise green space resource allocation, and improve the stability and function of the ecosystem. In this paper, the LSTM+ST-ConvNet model and other traditional spatiotemporal prediction models, ARIMA, XGBoost, and RF, compare the green area prediction from 2020 to 2024 to test the performance of each model in green area prediction. The prediction results are shown in Figure 3.

Figure 3 describes the predictions of green area in 2020–2024 by the LSTM+ ST-ConvNet model and the ARIMA, XGBoost, and random forest (RF) models in this paper, as well as the comparison with the actual green area. The actual green area shows an overall upward trend. The actual green area at the beginning of 2020 is 460 km^2, and it can rise to 600 km^2 in 2024. The model in this paper predicts that the green area can be 470 km^2 starting from 2020 and 640 km^2 in 2024. The error between the prediction of this model and the actual green area is only 50 km^2, which is the most accurate green area prediction among all models. Although there is a certain deviation between the prediction of the model and the actual green area data, its predicted trend and volatility are closest to the actual data. The prediction accuracy of other traditional models is slightly lower than that of the model in this paper. Although these models can also reflect the basic trends

and fluctuations of green area, compared with the model in this paper, the prediction values of these models have obvious deviations in certain periods, especially in 2023–2024. The model in this paper can use its long-term and short-term memory capabilities to maintain long-term memory of historical data, especially in the long-term trend and seasonal fluctuations of data. In contrast, the ARIMA model is limited by its linear assumption when dealing with long-term trends and is difficult to adapt to nonlinear complex changes. XGBoost and RF, as tree-based models, perform well in fitting training data, but are not accurate enough in capturing the time dependency in time series data, resulting in a decrease in their accuracy in long-term predictions.

This paper continues to add stability tests and uses 5-fold cross-validation to evaluate the generalisation ability of the LSTM+ST-ConvNet model. The results show that the average RMSE is stable at 5.2 km^2, which is better than ARIMA (7.8 km^2) and XGBoost (6.5 km^2).

To verify the adaptability of the model, Beijing (temperate continental climate, high industrial land use) and Chengdu (subtropical humid climate, high agricultural land use) were used as objects to predict the changes in green space areas from 2020 to 2024. The error of LSTM+ST-ConvNet in Beijing was 52 km^2 and in Chengdu was 48 km^2, both lower than ARIMA (75 km^2 in Beijing and 65 km^2 in Chengdu), proving its cross-regional applicability.

5.3 Comparative experiment on monitoring changes in green space coverage

To compare the performance of various modern models in monitoring the change of UGS coverage and verify the advantages of the proposed model ST-DBSCAN+GTWR in clustering accuracy, hotspot area identification, and operation efficiency, this experiment uses a multi-model comparison method to collect remote sensing image data of Guangzhou in 2024 and extract UGS coverage information. It trains RF, CNN, GNN, Transformer, and the proposed model respectively, calculates the green space coverage rate, Kappa coefficient, and running time indicators, and evaluates the performance of each model.

Figure 4 describes the performance comparison of each model in monitoring UGS coverage changes through three aspects: green space coverage, Kappa coefficient, and model running time. Sub-graph (a) describes the actual green coverage and the coverage of each model. The actual green coverage is 25.3%. The coverage monitored by the model in this paper is 25.2%, which is closest to the actual green coverage among the compared models. Sub-graphs (b) and (c) evaluate the accuracy and computational efficiency of hotspot area identification of each model based on the Kappa coefficient and model running time. The Kappa coefficient of the model in this paper is 0.92, and the running time is 15 minutes, which is 0.02 higher than the Kappa coefficient of the GNN model, and the model running time is 15 minutes faster. Experiments show that the proposed model has significant advantages in monitoring accuracy, hotspot identification, and operation efficiency.

Figure 4 Indicator comparison of each model, (a) each model and actual green space coverage, (b) Kappa coefficient comparison of each model, (c) running time comparison of each model (see online version for colours)

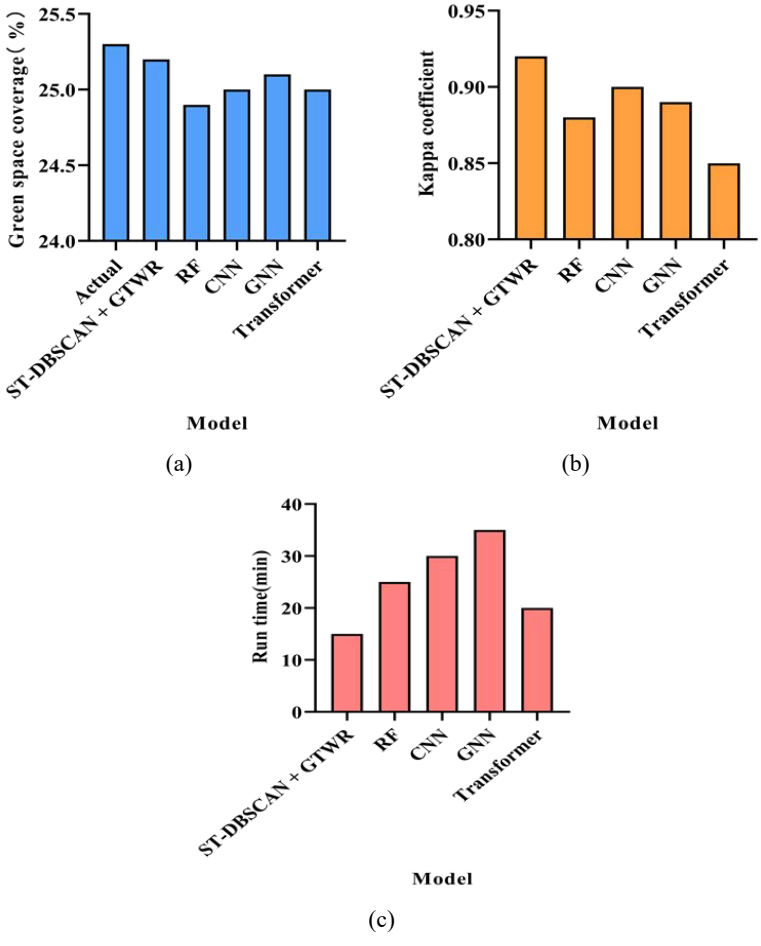

5.4 Evaluation of long-term sustainability of green landscape based on sustainability index

By establishing a sustainability index, combined with the green area, ecological function, and green change trend of different regions in Guangzhou, the long-term sustainability of green landscapes in various regions of Guangzhou is evaluated. The green change information of Tianhe District, Yuexiu District, Haizhu District, Baiyun District, Liwan District, Panyu District, Huangpu District, Huadu District, Conghua District, and Zengcheng District is selected. This paper compares the ecological service function scores and sustainability indexes of different regions to assess whether the green landscapes in the regions have good sustainability or may face the risk of green land degradation or ecological function decline, as shown in Figure 5.

Figure 5 Comparison of ecological service functions and sustainability index in different regions (see online version for colours)

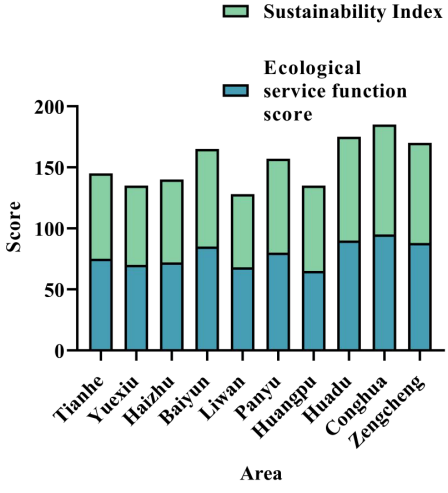

Figure 5 describes the comparison of ecological service functions and sustainability indexes of ten districts in Guangzhou. Liwan District has an ecological service function score of 68 and a sustainability index of 60, which is the lowest sustainability among the comparison areas. Conghua District has an ecological service function score of 95 and a sustainability index of 90, which is the highest sustainability. Tianhe District, Yuexiu District, Haizhu District, Liwan District, Huangpu District, and other areas with low sustainability are all major commercial and administrative centres of Guangzhou, while the other areas are suburban and remote areas with high sustainability. Experimental data show that the green space sustainability in the central city is relatively low, while the green space area in the suburbs is large, and the land development intensity is low, and the ecological service function and sustainability index of these areas are higher.

Although the central urban area has a high intensity of policy implementation, the policy effect is easily diluted by the urbanisation process due to the high intensity of land development and low stock of historical green space; while the suburbs achieve higher sustainability with lower policy input through the protection of ecological green space and intensive management of production green space. This shows that there is a spatial mismatch in the current policy effectiveness. In the future, it is necessary to strengthen the 'green space restoration compensation mechanism' for the central urban area and strengthen the 'ecological red line supervision' in the suburbs to optimise the allocation of policy resources.

The experimental results show that the green space change rate varies significantly among different cities, with Shenzhen and Shaoguan having high growth rates, while Zhuhai and Huizhou have lower growth rates. This is mainly related to regional development patterns, policy orientations, and natural conditions. Shenzhen's strong ecological restoration policies have promoted green space growth, while other cities have slowed down their growth rates due to infrastructure construction. The GTWR model analysis points out that there is spatiotemporal heterogeneity in the impact of population density and land development intensity on green space changes. Policy intervention in high-density areas can alleviate development pressure, while natural vegetation in

low-density areas is vulnerable to invasion. In addition, the sustainability index of urban areas is generally lower than that of suburbs, reflecting the problem of green space fragmentation caused by high-intensity development. The LSTM+ST-ConvNet model effectively captures the complex spatiotemporal characteristics of green space changes.

6 Conclusions

Based on the spatiotemporal analysis algorithm, this paper uses the ST-DBSCAN algorithm and the GTWR model to achieve high-precision monitoring of UGS coverage changes and spatiotemporal non-stationary analysis of driving factors, revealing the spatiotemporal differentiation of green space changes and their driving mechanisms. It combines the LSTM and ST-ConvNet models to predict the future evolution trend of green space landscapes and compares them with multiple prediction models based on the prediction results. The experiment shows that the prediction trend of this model is the most accurate, which provides a scientific basis for UGS planning. This study comprehensively evaluates the ecological, economic, and social benefits of green space through a multi-dimensional sustainability evaluation system, providing theoretical support for urban sustainable development. However, this study still has certain limitations, such as the limited spatiotemporal resolution of the data source, and the model's ability to describe complex driving factors needs to be further improved. Future research can combine sub-meter high-resolution satellite images to improve the accuracy of ST-DBSCAN in identifying the fragmentation process of small green patches, and use its richer spectral and texture information to optimise the spatiotemporal heterogeneity modelling of micro-driving factors in the GTWR model.

Acknowledgements

This work was supported by the 2023 youth project of the philosophy and Social Sciences Planning of Guangdong Province, 'construction and characteristics of landscape gene map of Wuyi traditional villages based on Rough Set Theory' No. GD23YYS17.

Declarations

All authors declare that they have no conflicts of interest.

References

Candra, D.S., Phinn, S. and Scarth, P. (2020) 'Cloud and cloud shadow masking for Sentinel-2 using multitemporal images in a global area', *International Journal of Remote Sensing*, Vol. 41, No. 8, pp.2877–2904.

Chen, W., Zhang, F., Zhu, Y. et al. (2022) 'Analysis of the impact of multiscale green landscape on urban PM2.5', *Air Quality, Atmosphere & Health*, Vol. 15, No. 8, pp.1319–1332.

Comber, A., Brunsdon, C., Charlton, M. et al. (2023) 'A route map for successful applications of geographically weighted regression', *Geographical Analysis*, Vol. 55, No. 1, pp.155–178.

Gao, S., He, D., Zhang, Z. et al. (2023) 'A novel dynamic interpolation method based on both temporal and spatial correlations', *Applied Intelligence*, Vol. 53, No. 5, pp.5100–5125.

García-Cabrera, R.D., Cuevas-Agulló, E., Barreto, Á. et al. (2020) 'Aerosol retrievals from the EKO MS-711 spectral direct irradiance measurements and corrections of the circumsolar radiation', *Atmospheric Measurement Techniques*, Vol. 13, No. 5, pp.2601–2621.

Ghalehteimouri, K.J., Ros, F.C. and Rambat, S. (2024) 'Flood risk assessment through rapid urbanization LULC change with destruction of urban green infrastructures based on NASA Landsat time series data: a case study of Kuala Lumpur between 1990–2021', *Ecological Frontiers*, Vol. 44, No. 2, pp.289–306.

Goovaerts, P., Rihana-Abdallah, A. and Pang, Y. (2024) 'Space-time distribution of trichloroethylene groundwater concentrations: geostatistical modeling and visualization', *Mathematical Geosciences*, Vol. 56, No. 3, pp.437–464.

He, Z., Deng, M., Cai, J. et al. (2020) 'Mining spatiotemporal association patterns from complex geographic phenomena', *International Journal of Geographical Information Science*, Vol. 34, No. 6, pp.1162–1187.

Howarth, J.D., Barth, N.C., Fitzsimons, S.J. et al. (2021) 'Spatiotemporal clustering of great earthquakes on a transform fault controlled by geometry', *Nature Geoscience*, Vol. 14, No. 5, pp.314–320.

Huang, S., Tang, L., Hupy, J.P. et al. (2021) 'A commentary review on the use of normalized difference vegetation index (NDVI) in the era of popular remote sensing', *Journal of Forestry Research*, Vol. 32, No. 1, pp.1–6.

Jian, Z. and Hao, S. (2020) 'Geo-spatial analysis and optimization strategy of park green space landscape pattern of Garden City – a case study of the central district of Mianyang City, Sichuan Province', *European Journal of Remote Sensing*, Vol. 53, No. 1, pp.309–315.

Kowe, P., Mutanga, O. and Dube, T. (2021) 'Advancements in the remote sensing of landscape pattern of urban green spaces and vegetation fragmentation', *International Journal of Remote Sensing*, Vol. 42, No. 10, pp.3797–3832.

Kuhlemann, L.M., Tetzlaff, D., Smith, A. et al. (2021) 'Using soil water isotopes to infer the influence of contrasting urban green space on ecohydrological partitioning', *Hydrology and Earth System Sciences*, Vol. 25, No. 2, pp.927–943.

Li, X.X., Tang, L.Y., Peng, W. et al. (2022) 'Estimation method of urban green space living vegetation volume based on backpack light detection and ranging. *Ying yong sheng tai xue bao = The Journal of Applied Ecology*, Vol. 33, No. 10, pp.2777–2784.

Lv, Z.Y., Huang, H.T., Li, X. et al. (2022) 'Land cover change detection with heterogeneous remote sensing images: review, progress, and perspective', *Proceedings of the IEEE*, Vol. 110, No. 12, pp.1976–1991.

Naikoo, M.W., Rihan, M. and Ishtiaque, M. (2020) 'Analyses of land use land cover (LULC) change and built-up expansion in the suburb of a metropolitan city: spatio-temporal analysis of Delhi NCR using landsat datasets', *Journal of Urban Management*, Vol. 9, No. 3, pp.347–359.

Nasehi, S. and Imanpour Namin, A. (2020) 'Assessment of urban green space fragmentation using landscape metrics (case study: district 2, Tehran city)', *Modeling Earth Systems and Environment*, Vol. 6, No. 4, pp.2405–2414.

Nouri, H., Nagler, P., Chavoshi Borujeni, S. et al. (2020) 'Effect of spatial resolution of satellite images on estimating the greenness and evapotranspiration of urban green spaces', *Hydrological Processes*, Vol. 34, No. 15, pp.3183–3199.

Roy, P.S., Ramachandran, R.M., Paul, O. et al. (2022) 'Anthropogenic land use and land cover changes – a review on its environmental consequences and climate change', *Journal of the Indian Society of Remote Sensing*, Vol. 50, No. 8, pp.1615–1640.

Tao, Z., Chen, J., Wu, W. et al. (2024) 'Spatiotemporal association of urban park characteristics and physical activity levels based on GTWR: a serial cross-sectional observational study', *Journal of Urban Management*, Vol. 13, No. 3, pp.398–409.

Westerholt, R. (2023) 'A simulation study to explore inference about global Moran's I with random spatial indexes', *Geographical Analysis*, Vol. 55, No. 4, pp.621–650.

Wu, S., Wang, Z., Du, Z. et al. (2021) 'Geographically and temporally neural network weighted regression for modeling spatiotemporal non-stationary relationships', *International Journal of Geographical Information Science*, Vol. 35, No. 3, pp.582–608.

Yang, B. (2020) 'Assessing spatial disparities and spatial-temporal dynamic of urban green spaces: a case study of city of Chicago', *Journal of the Korean Society of Surveying, Geodesy, Photogrammetry and Cartography*, Vol. 38, No. 5, pp.487–496.

Yu, H., Fotheringham, A.S., Li, Z. et al. (2020) 'Inference in multiscale geographically weighted regression', *Geographical Analysis*, Vol. 52, No. 1, pp.87–106.

Zakeri, F. and Saradjian, M.R. (2022) 'Change detection in multispectral images based on fusion of change vector analysis in posterior probability space and posterior probability space angle mapper', *Geocarto International*, Vol. 37, No. 5, pp.1450–1464.

Zhang, Y., An, H., Xing, Y. et al. (2023) 'Learning temporal and spatial features jointly: a unified framework for space-time data prediction in industrial IoT networks', *IEEE Sensors Journal*, Vol. 23, No. 16, pp.18752–18764.